Searching for New Physics with a Levitated-Sensor-Based Gravitational-Wave Detector

Nancy Aggarwal,[1,2] George P. Winstone,[1] Mae Teo,[3] Masha Baryakhtar,[4,5] Shane L. Larson,[2]
Vicky Kalogera,[2] and Andrew A. Geraci[1,2,*]

[1]*Center for Fundamental Physics, Department of Physics and Astronomy, Northwestern University, Evanston, Illinois 60208, USA*
[2]*Center for Interdisciplinary Exploration and Research in Astrophysics (CIERA), Department of Physics and Astronomy, Northwestern University, Evanston, Illinois 60208, USA*
[3]*Stanford Institute for Theoretical Physics, Stanford University, Stanford, California 94305, USA*
[4]*Center for Cosmology and Particle Physics, Department of Physics, New York University, New York, New York 10003, USA*
[5]*Department of Physics, University of Washington, Seattle, Washington 98195, USA*

(Received 25 October 2020; revised 13 November 2021; accepted 9 February 2022; published 16 March 2022)

The levitated sensor detector (LSD) is a compact resonant gravitational-wave (GW) detector based on optically trapped dielectric particles that is under construction. The LSD sensitivity has more favorable frequency scaling at high frequencies compared to laser interferometer detectors such as LIGO and VIRGO. We propose a method to substantially improve the sensitivity by optically levitating a multilayered stack of dielectric discs. These stacks allow the use of a more massive levitated object while exhibiting minimal photon recoil heating due to light scattering. Over an order of magnitude of unexplored frequency space for GWs above 10 kHz is accessible with an instrument 10 to 100 meters in size. Particularly motivated sources in this frequency range are gravitationally bound states of the axion from quantum chromodynamics with decay constant near the grand unified theory scale that form through black hole superradiance and annihilate to GWs. The LSD is also sensitive to GWs from binary coalescence of sub-solar-mass primordial black holes and as-yet unexplored new physics in the high-frequency GW window.

DOI: 10.1103/PhysRevLett.128.111101

Introduction.—Kilometer-scale ground-based gravitational-wave (GW) interferometers have recently opened a new field of astronomy by viewing the Universe in gravitational wave radiation, with remarkable sensitivity at frequencies ranging from 10 s of hertz to a few kilohertz [1]. Already, several exciting discoveries have resulted from these detectors, including the existence of binary black hole (BH) and neutron star systems [2]. In this new field it is imperative to extend the GW search to other frequencies, just as x-ray astronomy and radio astronomy have done for the electromagnetic spectrum. Many promising experiments and techniques for probing the GW spectrum, including pulsar timing arrays [3,4], atomic clocks and other interferometers [5,6], LISA [7,8], and DECIGO [9] focus on frequencies below those probed by ground-based interferometers. There are several proposals and initial bounds above the audio band, largely at frequencies of over 100 MHz [10–17], but few established methods to systematically probe the higher frequency part of the GW spectrum, where a variety of interesting sources could exist.

The high-frequency GW regime is particularly well suited for beyond-the-standard-model physics searches [18]. A unique high-frequency GW signal can be sourced by macroscopic bound states of axions around light astrophysical BHs [19,20]. The quantum chromodynamics (QCD) axion may explain the lack of charge-parity violation in the strong interactions [21–23] and is a dark matter candidate [24–26]. If an ultralight boson, such as the axion, has Compton wavelength of order the BH size, it is produced in exponentially large numbers through superradiance, forming a "gravitational atom." The axions produce coherent, monochromatic GW radiation [20,27]. For the theoretically well-motivated grand-unified-theory-scale QCD axion, the emission frequency is $\sim$100 kHz.

GWs could also open a window on the nature of dark matter (DM), a strong indicator for new physics [28–30]. Potential candidates include primordial black holes (PBHs). To date, ground-based interferometers have observed binary BHs with mass ranging from a few to a hundred solar masses, prompting renewed study of BH formation channels [31,32]. If BH binaries with chirp mass lower than 0.1 $M_\odot$—which generate GWs in the frequency range accessible by LSD—are observed, they are likely to be primordial in origin, forming part of the galactic DM. While the PBH mass spectrum is constrained from existing experiments [33–38], GW searches in the 10 kHz band provide an independent probe.

Other predicted sources of high frequency GWs include cosmological sources such as inflation [39,40], cosmic strings [41], axionic preheating [42,43], and phase transitions [44,45], as well as plasma instabilities [40] and other DM candidates [46].

In this Letter, we describe a levitated sensor detector (LSD) based on optically levitated multilayered dielectric microstructures. This technique can search for high frequency GWs in the band of ∼10–300 kHz, extending the frequency reach of existing instruments by over an order of magnitude. Unlike the ground-based interferometer observatories which are limited at high frequency by photon shot noise, our approach is limited at high frequency by thermal noise in the motion of the levitated particles and heating due to light scattering. The different frequency scaling of this noise makes the LSD competitive at high frequencies: while the sensitivity of ground-based interferometers like LIGO, VIRGO, and KAGRA decreases at higher frequency, the LSD sensitivity improves, enabling a substantial advance by a compact detector [47].

Optically levitated sensors for high-frequency GW detection were proposed in Ref. [47]. In this Letter we propose an extension particularly suited for GW detection: using a stack of thin-layered dielectric discs. Stacked disks address a major limiting quantum noise source of the levitated sensor technology—photon recoil heating—while at the same time increasing the mass of the levitated object, further increasing sensitivity. Photon recoil heating [48], recently observed in optical levitation experiments [49], raises the effective temperature of the levitated object and hence degrades force sensitivity [50]. It has been shown theoretically [47,51] that if a disc is levitated instead of a sphere, the heating rate can be lowered. The stacked disk approach could result in significant sensitivity improvements, depending on the shape and size of the levitated object. For the particular geometry we consider, we expect an improvement of over a factor of 20, leading to a $\sim 10^4$ increase in volumetric reach for GW sources.

Experimental setup and sensitivity.—We consider a compact Michelson interferometer configuration with Fabry-Pérot arms as shown in Fig. 1. A dielectric object is suspended at an anti-node of the standing wave inside each Fabry-Pérot arm. A second laser can be used to read out the position of the object as well as cool it along the cavity axes, as described for a similar setup in Ref. [47]. The optical potential for this trap is $U = (1/c) \int I(\vec{r})[\epsilon(\vec{r}) - 1] d^3\vec{r}$ where I is the laser intensity, ϵ is the relative dielectric constant, and the integration is performed over the extent of the dielectric particle. The trapping frequency along the axis of the cavity is determined by $\omega_0^2 = (1/M)(d^2U/dx^2)|_{x=x_s}$ for a sensor of mass M trapped at equilibrium position x_s.

A passing GW with frequency $\Omega_{\rm GW}$ imparts a force on the trapped particle [47], which is resonantly excited when $\omega_0 = \Omega_{\rm GW}$. Unlike a resonant-bar detector, ω_0 is widely tunable with laser intensity. The second cavity arm permits rejection of common mode noise, for example from technical laser noise or vibration.

The minimum detectable strain $h_{\rm limit}$ for a particle with center-of-mass (c.m.) temperature $T_{\rm CM}$ is approximately [47]

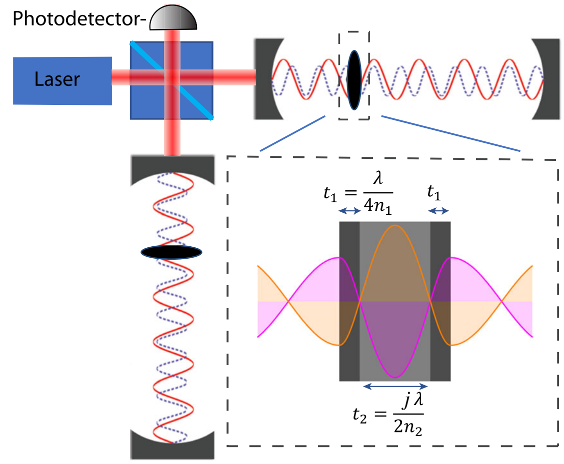

FIG. 1. Schematic of the levitated sensor detector (LSD) for GW detection at high frequencies. A stack of dielectric discs is optically confined in each Fabry-Pérot arm of a Michelson interferometer. A secondary beam (dotted line, not shown in inset) is used to cool and read out the motion of each stack along its respective cavity axis. Inset: electric field profile of the trapping light as it propagates through the dielectric stack supported in each arm of the interferometer, calculated using the method of Ref. [52]. The stack has high-index (n_1) end caps and a low-index (n_2) spacer with thicknesses t_1 and t_2, respectively. λ is the laser wavelength and j is an integer.

$$h_{\rm limit} = \frac{4}{\omega_0^2 L}\sqrt{\frac{k_B T_{\rm CM}\gamma_g b}{M}\left[1 + \frac{\gamma_{\rm sc}}{N_i\gamma_g}\right]}H(\omega_0), \quad (1)$$

where the cavity response function $H(\omega) \approx \sqrt{1 + 4\omega^2/\kappa^2}$ for a cavity of linewidth κ. Here, $N_i = k_B T_{\rm CM}/\hbar\omega_0$ is the mean initial phonon occupation number of the c.m. motion. $\gamma_g = (32P/\pi\bar{v}\rho t)$ is the gas damping rate at pressure P with mean gas speed $\bar{v}$ for a disc of thickness t and density ρ, and b is the bandwidth.

The photon recoil heating rate [47,51] $\gamma_{\rm sc} = (V_c\lambda\omega_0/4L)\{1/[\int dV(\epsilon - 1)]\}(1/\mathcal{F}_{\rm disc})$ is inversely proportional to the disc-limited finesse $\mathcal{F}_{\rm disc}$, i.e., 2π divided by the fraction of photons scattered by the disc outside the cavity mode. The integral is performed over the extent of the suspended particle. Here, V_c is the cavity mode volume [47]. While for a nanosphere the scattering and recoil is nearly isotropic [49], for a disc, if the beam size is smaller than the radius of the object and the wavefront curvature at the surface is small, the scattered photons acquire a stronger directional dependence and tend to be recaptured into the cavity mode. This reduces the variance of the recoil direction of the levitated object caused by the scattered photons.

Both of the damping rates that contribute to sensitivity in Eq. (1) scale inversely with the thickness of the levitated disc, for thickness smaller than radius. In the gas-dominated regime, $\gamma_{\rm sc} \ll N_i\gamma_g$, the sensitivity scales as

TABLE I. Experimental parameters for trapping of a 75 μm radius stack with 14.58 μm thick SiO_2 spacer (corresponding to $j = 28$) and quarter-wave 110 nm thick Si end caps in a cavity of length $L = 10$ m at $P = 10^{-11}$ Torr and room temperature. I_0 is the peak laser intensity striking the disc and $h_{\min} = h_{\text{limit}}/\sqrt{b}$ is the strain sensitivity where b is the measurement bandwidth.

Parameter	Units	$\omega_0/2\pi = 10$ kHz	$\omega_0/2\pi = 100$ kHz
λ	μm	1.5	1.5
P_{cavity}	W	0.486	48.6
I_0	W/m^2	2.2×10^8	2.2×10^{10}
$N_i\gamma_g$	Hz	1.7	0.17
γ_{sc}	Hz	0.005	0.05
$h_{\min}$	$1/\sqrt{\text{Hz}}$	7.6×10^{-21}	1.02×10^{-22}

$\sqrt{1/Mt}$ at fixed frequency. For sufficiently low vacuum, the sensitivity becomes photon-recoil-limited, and the strain sensitivity goes as $1/M\sqrt{\mathcal{F}_{\text{disc}}}$ [53].

We demonstrate that it is possible to increase the mass of the levitated object, and hence the sensitivity to GWs, without substantially increasing the photon recoil rate by using a *stacked* disc geometry. The thickness of each layer can be chosen to attain nearly perfect transmission, and the high-index sections serve as "handles" since they have a stronger affinity to the antinodes of an optical standing wave. Multiple reflections within the stack further enhance the optical trapping potential.

As a proof of principle, we consider a $a = 75$ μm radius dielectric stack in a three-layer configuration with high-index Si ($n_1 = 3.44$) end caps of thickness $t_1 = \lambda/4n_1$ on a low-index SiO_2 ($n_2 = 1.45$) spacer cylinder of length $j\lambda/2n_2$, where n_1 and n_2 are the index of refraction of the end caps and spacer, respectively, and j is an integer. Proposed experimental parameters are shown in Table I, for a trapping beam radius $w_0 = 37.5$ μm.

To estimate $\mathcal{F}_{\text{disc}}$ for the stack, we compute the 3D scattering using a finite element Greens dyadic method based on the pyGDM2 toolkit [54]. As a benchmark, we simulate SiO_2 discs and nanospheres and find them to agree with analytical limits. To determine $\mathcal{F}_{\text{disc}}$, we assume that the photons which scatter into twice the $1/e^2$ beam radius at the cavity end mirror are recaptured in the cavity mode, justified for the stack and beam radii considered here.

We show the results of the scattering simulations in Fig. 2. In Fig. 2(a) we show the distribution of scattered light in the far-field for a nanoparticle which acts as a point Rayleigh scatterer as well as for a dielectric stack of $a = 3$ μm, with $w_0 = a/2$. In Fig. 2(b), we show the resulting disc-limited finesse $\mathcal{F}_{\text{disc}}$ and beam divergence at the object surface for Si discs and Si/SiO_2 stacks for structures of varying radii. As expected, $\mathcal{F}_{\text{disc}}$ increases as the beam divergence decreases. The photon recoil scattering performance is not a sharp function of w_0/a, thus the requirement of $a = 2w_0$ need not be precisely satisfied. For our current setup of a $r = 75$ μm stack, we conservatively estimate $\mathcal{F}_{\text{disc}}$ as 4×10^4, the value calculated for a $a = 14$ μm disc. The $\mathcal{F}_{\text{disc}}$ calculation for larger radii is limited by computational memory, but our current results at smaller radii up to 14 μm indicate an increasing trend [see Fig. 2(b)]. The stack $\mathcal{F}_{\text{disc}}$ is large enough such that for our parameters, we stay in the gas-damping-limited regime, where the sensitivity is independent of $\mathcal{F}_{\text{disc}}$ and improves with both mass and thickness. In the photon-recoil-limited regime, the figure of merit $\mathcal{F}_{\text{disc}} \times M^2$ is shown in Fig 2(c). The better performance from using a stack comes from having a larger mass with a relatively small reduction in $\mathcal{F}_{\text{disc}}$.

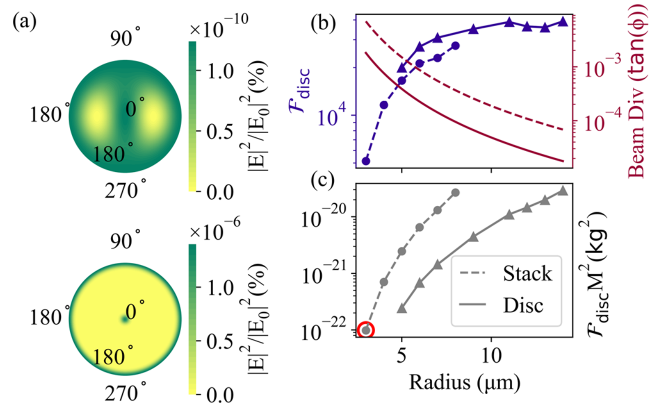

FIG. 2. (a) Top: far-field scattered light intensity distribution for a nanoparticle which acts as a pointlike Rayleigh scatterer; and (bottom) for a dielectric $Si/SiO_2/Si$ stack with $j = 1$ and radius 3 μm, where the laser beam waist is chosen to be one half the stack radius. (b) Disc-limited finesse $\mathcal{F}_{\text{disc}}$ and beam divergence angle ϕ at the object surface for Si discs (solid line) and $Si/SiO_2/Si$ stacks with $j = 1$ (dashed line) for varying radii. (c) $\mathcal{F}_{\text{disc}} \times M^2$ (figure of merit in the photon-recoil-dominated regime) vs radius. The red circled point corresponds to the stack considered in (a).

Results.—In Fig. 3 we show the estimated reach in strain sensitivity for the setup shown in Table I. The 300 kHz upper limit is chosen due to expected limitations from absorbed laser power by the suspended particle. In practice we estimate that the stack thicknesses need to be precise at the ∼1.5 and 0.5 nm level to ensure > 99% and 99.9% transmission, respectively. We assume vacuum of 10^{-11} Torr and room temperature for all cases except we assume cryogenic (4 K) for an optimized 100-m facility. The vast improvement relative to the scheme originally proposed in Ref. [47] can be seen by comparing the "disc" and "stack" curves for a 1-m instrument. For the proposed 100-m scheme, using a hybrid fiber-based approach as suggested in Ref. [55] may eliminate the need for meter-scale cavity end mirrors, provided fiber-related noise sources such as Brillouin scattering can be mitigated to a sufficient level. For our parameters which yield minimal recoil heating, the sensitivity remains in the

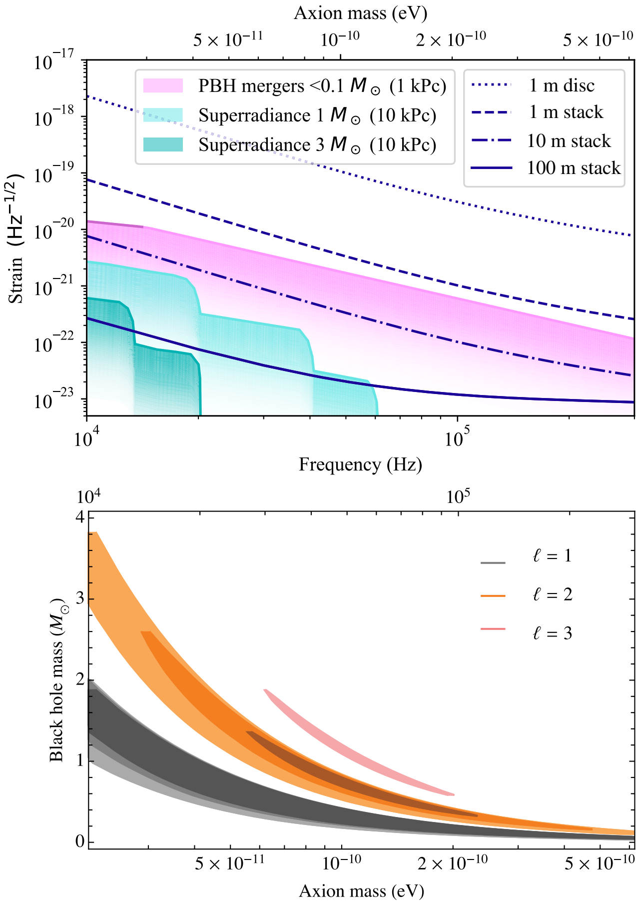

FIG. 3. Upper: strain sensitivity for optically levitated microdiscs (dotted) or stacked discs (dashed), at design sensitivity for the 1-m prototype instrument. The sensitivity curves are formed as the locus of the minima of the sensitivity from a single realization of the tunable optical trap frequency. The cyan shaded regions denote predicted signals due to GWs produced from axions around BHs in our galaxy within 10 kpc for 10^6 s coherent integration time. The pink area shows the expected strain from inspiraling and merging PBHs at distances ≥ 1 kpc. Also shown is projected sensitivity for a future 10-m room-temperature (dash-dotted) and 100-m cryogenic setup (solid). Cavity finesse $\mathcal{F} \approx \pi c/(L\kappa) = 10$ in all cases shown. Lower: reach at SNR = 1 to angle-averaged axion annihilation signals of the 100-m stack LSD setup. The shaded regions indicate where the reach exceeds 10 (light), 30 (medium), 50 (dark) kpc for a BH with initial spin $a_* = 0.9$ as a function of axion and BH mass. The three bands correspond to the $\ell = m = \{1, 2, 3\}$ SR levels. The $\ell = 3$ level exceeds only 10 kpc.

gas-damping-dominated regime despite the relatively large mass of the levitated particle. Improved sensitivity is possible in a 4K instrument where the main dissipation is due to background collisions with cryogenic gas molecules, resulting in a lower c.m. temperature without simultaneously reducing the mechanical quality factor. While optical absorption poses a challenge, cryogenic operation could be enabled either by using low-loss material comparable to high quality SiO_2 fiber ($\mathcal{I}m[\epsilon] \approx 10^{-10}$), or active solid-state laser cooling of the levitated particles [56] (see Supplemental Material [57]). Since LSD is a resonant detector, we show the strain sensitivity in Fig. 3 as the locus of best sensitivity for each tuned configuration. The resonant width (i.e., detector Q) is tunable via laser cooling as discussed in Ref. [47], and h_{limit} is Q independent given sufficient displacement sensitivity [47]. Readout noise, including photon shot noise, is expected to be subdominant, but affects the bandwidth of sensitivity for a given tuning of the instrument, as further described in the Supplemental Material [57]. With suitable vibration isolation, at frequencies above 10 kHz, limitations from seismic noise, gravity-gradient noise, and mirror and coating thermal noise are expected to be subdominant (see Supplemental Material [57]). Figure 3 also shows the predicted signals from BH superradiance and PBH inspirals and mergers.

Sensitivity to primordial black holes.—The pink area in Fig. 3 shows the expected GW strain from inspiraling and merging PBHs at a distance of 1 kpc. The dark pink line shows the strain from the inspiral of two 0.1 $M_\odot$ BHs and terminates at ~14.4 kHz, the GW frequency corresponding to the innermost stable circular orbit of the binary. Binaries of lighter BHs merge at higher frequencies, and the locus of their innermost stable circular orbit frequencies forms the boundary of the possible PBH signal space, shown in pink. Weaker signals from earlier inspiral stages, farther source distances and suboptimal source orientations form the shaded area. The 10-m instrument will be sensitive to PBHs ~ kpc away, and the 100-m instrument will be sensitive to PBHs more than 10 kpc away.

Sensitivity to black hole superradiance.—The frequency range probed by LSD makes it sensitive to signals from ultralight bosons produced via BH superradiance. The angular momentum and energy of rotating astrophysical BHs can be converted into gravitationally bound states of exponentially large numbers of ultralight bosons through BH superradiance [19,20,27,77–91]. The resulting "gravitational atom" has bound levels with angular momentum $\hbar\ell$ per axion.

Axions from a single level annihilate, sourcing continuous, monochromatic GWs with angular frequency of approximately twice the axion rest energy μ, $f_{\text{GW}} \simeq (\mu/\pi\hbar) \simeq 145\ \text{kHz}[\mu/(3\times 10^{-10}\ \text{eV})]$ [19,20]. While searches with LIGO and VIRGO data are under way for bosons with rest energy up to 4×10^{-12} eV [92–96], high-frequency detectors are necessary to observe the annihilation signal from theoretically well-motivated QCD axions with decay constant f_a near the grand-unified-theory scale, $\mu \simeq 3 \times 10^{-10}\ \text{eV}\ (2 \times 10^{16}\ \text{GeV}/f_a)$.

Figure 3 (upper) shows the maximum integrated strain of axion annihilation signals $ht_{\text{int}}^{1/2}$ from a BH within 10 kpc with initial spin $a_*^{\text{init}} = 0.9$, assuming a coherent integration time of $t_{\text{int}} = 10^6$ s. The envelope consists of angular momentum levels $\ell = 1$, 2, and 3, with $\ell = 3$ reaching higher axion masses, and BH masses of 1 $M_\odot$ and 3 $M_\odot$, with weaker signals arising from more distant and heavier BHs. See Supplemental Material [57] for further details.

In Fig. 3 (lower) we show the LSD reach for annihilation signals. Heavier axions can only form clouds of a given angular momentum around relatively lighter BHs while at fixed BH mass, heavier axions can form clouds only in levels with higher ℓ. As there is thought to be a gap in compact object masses with no BHs of $M_{\rm BH} \lesssim 5\ M_\odot$ formed [97–100] (although see new evidence of mass-gap compact objects [101–103]), it is particularly interesting to search for signals from $\ell > 1$ to reach new, heavier axion parameter space.

Discussion.—Current GW observatories such as advanced LIGO and VIRGO do not search for GWs over 10 kHz. Our approach enables a search for well-motivated beyond the standard model sources of GWs such as the grand-unified-theory-scale QCD axion, which could naturally exist at these frequencies. Looking forward, the few kilohertz frequency band is the prime region for GW emission from the postmerger dynamics of the compact object resulting from a binary neutron star inspirals [104,105]. Using even larger levitated masses could lead to further sensitivity improvements, enabling deeper exploration of physics such as the neutron star equation of state. The approach we describe will have a major discovery potential in uncharted GW frequency parameter space.

We would like to thank A. Arvanitaki and P. Barker for useful discussions. M. B. is supported by the James Arthur Postdoctoral Fellowship. M. T. is partially supported by the Stanford Physics Department Fellowship. A. G., G. W., and N. A. are supported in part by NSF Grants No. PHY-1806686 and No. PHY-1806671, the Heising-Simons Foundation, the John Templeton Foundation, and ONR Grant No. N00014-18-1-2370. A. G. and S. L. are supported by the W. M. Keck Foundation. V. K. is supported by a CIFAR Senior Fellowship and through Northwestern University through the D. I. Linzer Distinguished University Professorship. N. A. is also supported by the CIERA Postdoctoral Fellowship from the Center for Interdisciplinary Exploration and Research in Astrophysics at Northwestern University. This work used the Extreme Science and Engineering Discovery Environment (XSEDE) at the Pittsburgh Supercomputing Center through allocation TG-PHY190038, and the Quest computing facility at Northwestern.

N. A. and G. W. contributed to the optical trapping calculations. M. T., M. B., and N. A. estimated sources. A. G., S. L., and V. K. supervised the project. All authors contributed to discussions and writing.

[*]Corresponding author.
andrew.geraci@northwestern.edu

[1] B. P. Abbott *et al.*, Phys. Rev. Lett. **116**, 061102 (2016).
[2] B. P. Abbott *et al.* (LIGO Scientific and Virgo Collaborations), Phys. Rev. X **9**, 031040 (2019).
[3] G. Hobbs and S. Dai, Natl. Sci. Rev. **4**, 707 (2017).
[4] A. Weltman, P. Bull, S. Camera, K. Kelley, H. Padmanabhan, J. Pritchard, A. Raccanelli, S. Riemer-Srensen, L. Shao, S. Andrianomena *et al.*, Pub. Astron. Soc. Aust. **37**, e002 (2020).
[5] S. Kolkowitz, I. Pikovski, N. Langellier, M. D. Lukin, R. L. Walsworth, and J. Ye, Phys. Rev. D **94**, 124043 (2016).
[6] J. Coleman (MAGIS-100 Collaboration), Proc. Sci., ICHEP2018 08 (**2019**) 021 [arXiv:1812.00482].
[7] P. A. Seoane *et al.* (eLISA Collaboration), arXiv: 1305.5720.
[8] P. Amaro-Seoane *et al.*, arXiv:1702.00786.
[9] S. Kawamura *et al.*, Int. J. Mod. Phys. D **28**, 1845001 (2019).
[10] A. S. Chou, R. Gustafson, C. Hogan, B. Kamai, O. Kwon, R. Lanza, S. L. Larson, L. McCuller, S. S. Meyer, J. Richardson, C. Stoughton, R. Tomlin, and R. Weiss (Holometer Collaboration), Phys. Rev. D **95**, 063002 (2017).
[11] T. Akutsu, S. Kawamura, A. Nishizawa, K. Arai, K. Yamamoto, D. Tatsumi, S. Nagano, E. Nishida, T. Chiba, R. Takahashi, N. Sugiyama, M. Fukushima, T. Yamazaki, and M.-K. Fujimoto, Phys. Rev. Lett. **101**, 101101 (2008).
[12] A. M. Cruise and R. M. J. Ingley, Classical Quantum Gravity **23**, 6185 (2006).
[13] A. M. Cruise, Classical Quantum Gravity **29**, 095003 (2012).
[14] S. M. Vermeulen, L. Aiello, A. Ejlli, W. L. Griffiths, A. L. James, K. L. Dooley, and H. Grote, Classical Quantum Gravity **38**, 085008 (2021).
[15] A. Nishizawa, S. Kawamura, T. Akutsu, K. Arai, K. Yamamoto, D. Tatsumi, E. Nishida, M.-a. Sakagami, T. Chiba, R. Takahashi, and N. Sugiyama, Phys. Rev. D **77**, 022002 (2008).
[16] A. Ito, T. Ikeda, K. Miuchi, and J. Soda, Eur. Phys. J. C **80**, 1 (2020).
[17] A. Ejlli, D. Ejlli, A. M. Cruise, G. Pisano, and H. Grote, Eur. Phys. J. C **79**, 1 (2019).
[18] N. Aggarwal, O. Aguiar, A. Bauswein, G. Cella, S. Clesse, A. Cruise, V. Domcke, D. Figueroa, A. Geraci, M. Goryachev *et al.*, arXiv:2011.12414.
[19] A. Arvanitaki, S. Dimopoulos, S. Dubovsky, N. Kaloper, and J. March-Russell, Phys. Rev. D **81**, 123530 (2010).
[20] A. Arvanitaki and S. Dubovsky, Phys. Rev. D **83**, 044026 (2011).
[21] R. D. Peccei and H. R. Quinn, Phys. Rev. Lett. **38**, 1440 (1977).
[22] S. Weinberg, Phys. Rev. Lett. **40**, 223 (1978).
[23] F. Wilczek, Phys. Rev. Lett. **40**, 279 (1978).
[24] J. Preskill, M. B. Wise, and F. Wilczek, Phys. Lett. **120B**, 127 (1983).
[25] L. F. Abbott and P. Sikivie, Phys. Lett. **120B**, 133 (1983).
[26] M. Dine and W. Fischler, Phys. Lett. **120B**, 137 (1983).
[27] A. Arvanitaki, M. Baryakhtar, and X. Huang, Phys. Rev. D **91**, 084011 (2015).
[28] J. L. Feng, Annu. Rev. Astron. Astrophys. **48**, 495 (2010).

[29] G. Bertone, D. Hooper, and J. Silk, Phys. Rep. **405**, 279 (2005).
[30] S. Profumo, *An Introduction to Particle Dark Matter* (World Scientific, Singapore, 2017).
[31] M. Sasaki, T. Suyama, T. Tanaka, and S. Yokoyama, Phys. Rev. Lett. **117**, 061101 (2016).
[32] M. Sasaki, T. Suyama, T. Tanaka, and S. Yokoyama, Classical Quantum Gravity **35**, 063001 (2018).
[33] M. Zumalacárregui and U. c. v. Seljak, Phys. Rev. Lett. **121**, 141101 (2018).
[34] P. Tisserand *et al.* (The EROS-2 Collaboration), Astron. Astrophys. **469**, 387 (2007).
[35] C. Alcock *et al.* (The MACHO Collaboration), Astrophys. J. **550**, L169 (2001).
[36] EROS and MACHO Collaborations, Astrophys. J. Lett. **499**, L9 (1998).
[37] B. P. Abbott *et al.* (LIGO Scientific and the Virgo Collaborations), Phys. Rev. Lett. **123**, 161102 (2019).
[38] A. Miller, N. Aggarwal, S. Cless, and F. De Lillo, arXiv:2110.06188.
[39] N. Barnaby and M. Peloso, Phys. Rev. Lett. **106**, 181301 (2011).
[40] A. M. Cruise, Classical Quantum Gravity **29**, 095003 (2012).
[41] P. Ade *et al.* (Planck Collaboration), Astron. Astrophys. **571**, A25 (2014).
[42] D. G. Figueroa and F. Torrenti, J. Cosmol. Astropart. Phys. 10 (2017) 057.
[43] C. Caprini and D. G. Figueroa, Classical Quantum Gravity **35**, 163001 (2018).
[44] M. Kamionkowski, A. Kosowsky, and M. S. Turner, Phys. Rev. D **49**, 2837 (1994).
[45] I. Garcia Garcia, S. Krippendorf, and J. March-Russell, Phys. Lett. B **779**, 348 (2018).
[46] H.-K. Guo, K. Riles, F.-W. Yang, and Y. Zhao, Commun. Phys. **2**, 155 (2019).
[47] A. Arvanitaki and A. A. Geraci, Phys. Rev. Lett. **110**, 071105 (2013).
[48] J. P. Gordon and A. Ashkin, Phys. Rev. A **21**, 1606 (1980).
[49] V. Jain, J. Gieseler, C. Moritz, C. Dellago, R. Quidant, and L. Novotny, Phys. Rev. Lett. **116**, 243601 (2016).
[50] A. A. Geraci, S. B. Papp, and J. Kitching, Phys. Rev. Lett. **105**, 101101 (2010).
[51] D. E. Chang, K.-K. Ni, O. Painter, and H. J. Kimble, New J. Phys. **14**, 045002 (2012).
[52] S. J. Byrnes, arXiv:1603.02720.
[53] For these scalings we have assumed a similar density throughout the levitated object.
[54] P. R. Wiecha, Comput. Phys. Commun. **233**, 167 (2018).
[55] A. Pontin, L. S. Mourounas, A. A. Geraci, and P. F. Barker, New J. Phys. **20**, 023017 (2018).
[56] A. T. M. A. Rahman and P. F. Barker, Nat. Photonics **11**, 634 (2017).
[57] See Supplemental Material at http://link.aps.org/supplemental/10.1103/PhysRevLett.128.111101 for a discussion of additional noise sources, considerations for cryogenic operation, and an elaboration on the potential expected signals from black hole superradiance, which includes Refs. [58–76].
[58] E. D. Black, A. Villar, K. Barbary, A. Bushmaker, J. Heefner, S. Kawamura, F. Kawazoe, L. Matone, S. Meidt, S. R. Rao, K. Schulz, M. Zhang, and K. G. Libbrecht, Phys. Lett. A **328**, 1 (2004).
[59] T. Chalermsongsak, F. Seifert, E. D. Hall, K. Arai, E. K. Gustafson, and R. X. Adhikari, Metrologia **52**, 17 (2015).
[60] A. Schroeter *et al.*, arXiv:0709.4359.
[61] G. Cole, Crystalline Mirror Solutions, Inc., http://www.thorlabs.com (2021).
[62] J. Franc, N. Morgado, R. Flaminio, R. Nawrodt, I. Martin, L. Cunningham, A. Cumming, S. Rowan, and J. Hough, arXiv:0912.0107.
[63] Y. Hadjar, P. F. Cohadon, C. G. Aminoff, M. Pinard, and A. Heidmann, Europhys. Lett. **47**, 545 (1999).
[64] T. Seberson and F. Robicheaux, Phys. Rev. A **99**, 013821 (2019).
[65] F. van der Laan, F. Tebbenjohanns, R. Reimann, J. Vijayan, L. Novotny, and M. Frimmer, Phys. Rev. Lett. **127**, 123605 (2021).
[66] M. A. Bourebrab, D. T. Oben, G. G. Durand, P. G. Taylor, J. I. Bruce, A. R. Bassindale, and A. Taylor, J. Solgel Sci. Technol. **88**, 430 (2018).
[67] E. Hebestreit, R. Reimann, M. Frimmer, and L. Novotny, Phys. Rev. A **97**, 043803 (2018).
[68] F. Monteiro, S. Ghosh, A. G. Fine, and D. C. Moore, Phys. Rev. A **96**, 063841 (2017).
[69] G. Pagano, P. W. Hess, H. B. Kaplan, W. L. Tan, P. Richerme, P. Becker, A. Kyprianidis, J. Zhang, E. Birckelbaw, M. R. Hernandez, Y. Wu, and C. Monroe, Quantum Sci. Technol. **4**, 014004 (2018).
[70] M. Schwarz, O. O. Versolato, A. Windberger, F. R. Brunner, T. Ballance, S. N. Eberle, J. Ullrich, P. O. Schmidt, A. K. Hansen, A. D. Gingell, M. Drewsen, and J. R. C. Lopez-Urrutia, Rev. Sci. Instrum. **83**, 083115 (2012).
[71] U. Delić, M. Reisenbauer, K. Dare, D. Grass, V. Vuletić, N. Kiesel, and M. Aspelmeyer, Science **367**, 892 (2020).
[72] B. Abbott *et al.*, New J. Phys. **11**, 073032 (2009).
[73] S. D. Melgaard, A. R. Albrecht, M. P. Hehlen, and M. Sheik-Bahae, Sci. Rep. **6**, 20380 (2016).
[74] M. Baryakhtar, M. Galanis, R. Lasenby, and O. Simon, Phys. Rev. D **103**, 095019 (2021).
[75] H. Yoshino and H. Kodama, Prog. Theor. Exp. Phys. **2014**, 043E02 (2014).
[76] A. Gruzinov, arXiv:1604.06422.
[77] T. Damour, N. Deruelle, and R. Ruffini, Lett. Nuovo Cimento **15**, 257 (1976).
[78] I. M. Ternov, V. R. Khalilov, G. A. Chizhov, and A. B. Gaina, Izv. Vuz. Fiz. **21N9**, 109 (1978) [Sov. Phys. J. **21**, 1200 (1978)].
[79] T. J. M. Zouros and D. M. Eardley, Ann. Phys. (N.Y.) **118**, 139 (1979).
[80] S. L. Detweiler, Phys. Rev. D **22**, 2323 (1980).
[81] R. Brito, V. Cardoso, and P. Pani, Classical Quantum Gravity **32**, 134001 (2015).
[82] R. Brito, V. Cardoso, and P. Pani, Lect. Notes Phys. **906**, 1 (2015).
[83] A. Arvanitaki, M. Baryakhtar, S. Dimopoulos, S. Dubovsky, and R. Lasenby, Phys. Rev. D **95**, 043001 (2017).
[84] R. Brito, S. Ghosh, E. Barausse, E. Berti, V. Cardoso, I. Dvorkin, A. Klein, and P. Pani, Phys. Rev. Lett. **119**, 131101 (2017).

[85] R. Brito, S. Ghosh, E. Barausse, E. Berti, V. Cardoso, I. Dvorkin, A. Klein, and P. Pani, Phys. Rev. D **96**, 064050 (2017).

[86] D. Baumann, H. S. Chia, and R. A. Porto, Phys. Rev. D **99**, 044001 (2019).

[87] P. Pani, V. Cardoso, L. Gualtieri, E. Berti, and A. Ishibashi, Phys. Rev. D **86**, 104017 (2012).

[88] H. Witek, V. Cardoso, A. Ishibashi, and U. Sperhake, Phys. Rev. D **87**, 043513 (2013).

[89] M. Baryakhtar, R. Lasenby, and M. Teo, Phys. Rev. D **96**, 035019 (2017).

[90] W. E. East, Phys. Rev. D **96**, 024004 (2017).

[91] N. Siemonsen and W. E. East, Phys. Rev. D **101**, 024019 (2020).

[92] L. Tsukada, T. Callister, A. Matas, and P. Meyers, Phys. Rev. D **99**, 103015 (2019).

[93] V. Dergachev and M. A. Papa, Phys. Rev. D **101**, 022001 (2020).

[94] C. Palomba, S. D'Antonio, P. Astone, S. Frasca, G. Intini, I. La Rosa, P. Leaci, S. Mastrogiovanni, A. L. Miller, F. Muciaccia, O. J. Piccinni, L. Rei, and F. Simula, Phys. Rev. Lett. **123**, 171101 (2019).

[95] S. J. Zhu, M. Baryakhtar, M. A. Papa, D. Tsuna, N. Kawanaka, and H.-B. Eggenstein, Phys. Rev. D **102**, 063020 (2020).

[96] L. Sun, R. Brito, and M. Isi, Phys. Rev. D **101**, 063020 (2020); **102**, 089902(E) (2020).

[97] C. D. Bailyn, R. K. Jain, P. Coppi, and J. A. Orosz, Astrophys. J. **499**, 367 (1998).

[98] F. Ozel, D. Psaltis, R. Narayan, and J. E. McClintock, Astrophys. J. **725**, 1918 (2010).

[99] L. Kreidberg, C. D. Bailyn, W. M. Farr, and V. Kalogera, Astrophys. J. **757**, 36 (2012).

[100] K. Belczynski, G. Wiktorowicz, C. L. Fryer, D. E. Holz, and V. Kalogera, Astrophys. J. **757**, 91 (2012).

[101] R. Abbott *et al.* (LIGO Scientific, Virgo Collaborations), Astrophys. J. Lett. **896**, L44 (2020).

[102] T. A. Thompson, C. S. Kochanek, K. Z. Stanek, C. Badenes, R. S. Post, T. Jayasinghe, D. W. Latham, A. Bieryla, G. A. Esquerdo, P. Berlind, M. L. Calkins, J. Tayar, L. Lindegren, J. A. Johnson, T. W.-S. Holoien, K. Auchettl, and K. Covey, Science **366**, 637 (2019).

[103] B. Margalit and B. D. Metzger, Astrophys. J. Lett. **850**, L19 (2017).

[104] A. Bauswein and H.-T. Janka, Phys. Rev. Lett. **108**, 011101 (2012).

[105] M. Oertel, M. Hempel, T. Klähn, and S. Typel, Rev. Mod. Phys. **89**, 015007 (2017).